River Meandering

Proceedings of the Conference Rivers '83

Sponsored by the
Waterway, Port, Coastal and Ocean Division
of the American Society of Civil Engineers

In cooperation with
International Association for Hydraulic Research
U.S. Army Corps of Engineers
Louisiana Section, ASCE
New Orleans Branch, ASCE

New Orleans, Louisiana
October 24-26, 1983

Charles M. Elliott, Editor

Published by the
American Society of Civil Engineers
345 East 47th Street
New York, New York 10017-2398

18

BOUNDARY SHEAR STRESS, SEDIMENT TRANSPORT AND BED MORPHOLOGY IN A SAND-BEDDED RIVER MEANDER DURING HIGH AND LOW FLOW

W.E. Dietrich* J.D. Smith† and T. Dunne††

ABSTRACT

In a small sand-bedded river-meander, velocity, boundary shear stress, water surface topography, bedload, bedform and suspended load transport fields were mapped during spring snowmelt season over a four-year period, 1976-1979. Discharge, controlled by irrigation outflow, was about 0.7 bankfull flow in three of the years. In the drought year, 1977, the discharge was only about 0.2 bankfull. At the higher stage, the total boundary shear stress, computed from the depth-slope product, was 55 dynes/cm^2. Velocity profile measurements over mobile bedforms indicate that the average boundary shear stress resulting from resistance due to form drag over bedforms as well as resistance from mobile and stationary bed particles was 30 dynes/cm^2. We also computed the boundary shear stress causing bedload transport with a recently developed model that uses single-velocity measurements near the bed, and at the high stage, this averaged about 15 dynes per cm^2 near the bedform crests. For the lower flow, the total boundary shear stress was about 26 dynes/cm while bedform and bedload boundary shear stress averaged about 22 dynes/cm^2. The boundary shear stress responsible for bedload transport alone was on average about 12 dynes/cm^2 in this case. Although there was a reduction by one-half in the total boundary shear stress with reduced stage, the boundary shear stress available for bedload transport decreased by only 25%. Commensurately the total bedload transport decreased by only about one-half from 129 to 58 gm/sec. During lower flow, net deposition in the pool and erosion on the flank of the high stage point bar formed a bed morphology geometrically similar to the high flow form. This produced a distinct flat-topped point bar cut into the convex bank of the high stage sand reducing the amplitude of the point bar relative to the width and radius of curvature, thus decreasing the proportion of total boundary shear stress associated with large scale bar resistance. As a consequence, proportionately more of the total boundary shear stress was available for sediment transport at low flow. Similarities in crest height to wavelength ratios of the mobile bedforms at high and low stage led to the same ratio of bedform to bedload-transporting boundary shear stresses. This ratio, equal to about two, is predicted by the Smith-McLean equation. As in the high flow case, the zone of high bedload transport follows the outward shifting zone of maximum boundary shear stress through the bend, and the bedload transport field can be predicted accurately using the local boundary shear stress values in the Yalin bedload equation.

Introduction

The bedform morphology of sand-bedded rivers changes continuously with stage fluctuations. Not only do bedforms such as sandwaves and dunes adjust their form to changing flow conditions, but also large-scale features such as bars and pools alter their geometry. These changes may significantly affect the magnitude of the boundary shear stress available for bedload transport and, in more practical terms, the navigability of rivers. Understanding how large-scale bed modification occurs with stage fluctuations is an important step toward delineating the processes that ultimately control equilibrium bed morphology.

Two examples of cross-sectional changes in river meanders are illustrated in Figs. 1 and 2. Anding and Pierce (1) mentioned that an important concern on the Mississippi River is the tendency for point bars in sharp bends to build toward the outside bank during falling and low stages. Figure 1 shows that during a rising stage on a Mississippi River bend, the flow may erode at least partially the aggraded pool and point bar face and deposit sediment on the point bar top. At this particular site a chute channel also tended to form near the inside bank (1). At a much smaller scale, the same pattern of deposition and erosion occurs during stage change

*Department of Geology and Geophysics, University of California, Berkeley, CA 94720; †Geophysics Program, and ††Department of Geological Sciences, University of Washington, Seattle, WA 98195.

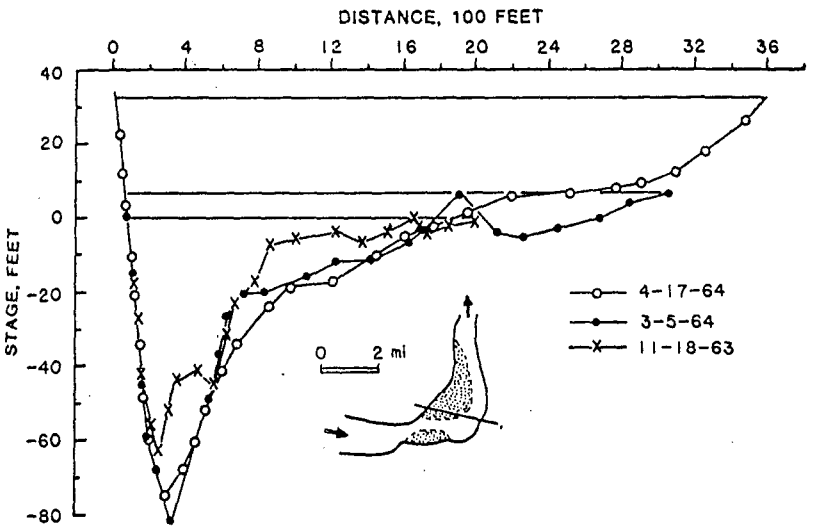

Fig. 1. - Changes in cross-sectional form with stage in the Ajax Bend Study Reach, Mississippi River (2). Symbols are to denote separate lines, not to indicate place of measurement.

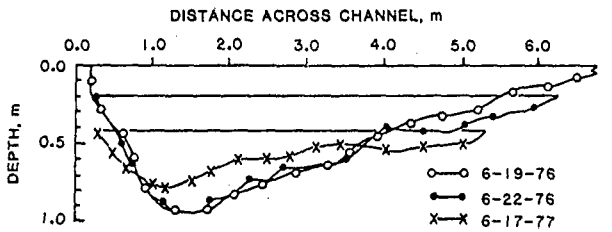

Fig. 2 - Changes in cross-sectional form with stage in the Muddy Creek, Wyoming study bend (4-7). Symbols are to denote separate lines, not to indicate place of measurement.

on Muddy Creek, Wyoming. Fig. 2 demonstrates that during a falling stage the point bar top is eroded and the point bar face and pool aggrades. In both channels the general cross-sectional form is preserved by a systematic pattern of erosion and deposition.

The purpose of this paper is to explore the consequences of bed morphology adjustment on the magnitude and distribution boundary shear stress and bedload transport at high and low flow in a sand-bedded river meander.

Study Site and Field Methods

Muddy Creek is a lowland tributary to the Upper Green River in western Wyoming. During the spring snowmelt runoff irrigation outflow is diverted into the channel providing long periods of nearly constant discharge. For three of the four years between 1976-1979, this discharge was about 1.1 m^3/sec, and in those years the bed morphology through the study reach was identical. Channel and flow properties were measured carefully during these high flow years and the measurement procedures are described elsewhere (4-7).

In 1977, drought conditions prevented significant irrigation and the flow was considerably lower, equal to about 0.3 m^3/sec. As illustrated in Fig. 2, the low flow conditions led to substantial morphological changes in the channel. In this low flow year, the discharge was less stable; for example, during the 10 day study period a brief rainstorm caused the stage to rise rapidly by 9 cm and then decline over two days to the original flow level. Measurements reported here were made before and after this discharge fluctuation when the stage was comparable. The brief fluctuation caused no major changes in the bed topography so the field data apparently record processes in near-balance with channel form.

Boundary Shear Stress

The boundary shear stresses corresponding to three scales of resistance in the channel were evaluated. An approximation for the pattern of total boundary shear stress, τ_{bt}, was computed using detailed measurements of water surface topography (see Fig. 3) and flow depth in combination with

$$\tau_{bt} = \rho g h S \tag{1}$$

Here ρ and g are the fluid density and gravitational acceleration, respectively, h is the depth of flow at a position on the bed and S is the downstream slope of the water surface corresponding to the depth-measurement. As noted by us in a separate paper in this volume, Eq. (1) does not include convective acceleration terms and may therefore provide poor predictions of the patterns of total boundary shear stress (see also, 4, 5). As input to Eq. 1 the water surface was surveyed at high flow with a level and with a rod by a person wading the stream (6); whereas at low flow this was done with a point gage mounted over the stream on an aluminum "I" beam and with a level sighting on a rod held at the water surface by a person standing on a wooden bridge. The errors incurred by the former method are discussed elsewhere (6).

The boundary shear stress, τ_{bf}, associated with resistance generated by mobile bedform (dunes, sandwaves and ripples), bed particle motion, and stationary grains (skin friction), was computed from velocity profiles made at dune crests with electromagnetic current meters. For the low-flow year, the analysis was the same as the high flow (4,5), but the current meter differed. During this experiment a 9 mm diameter, spherical, two-component electromagnetic current-meter mounted on a top-setting wading rod and held from a bridge was used to make velocity measurements in a zone 2 to 5 cm above the bed. In this near-boundary zone, the flow tends to be approximately steady and uniform, hence the "law of wall" can be used to compute boundary shear stress:

$$u = \frac{u_*}{\kappa} \ln z/z_f \tag{2}$$

$$\tau_{bf} \equiv \rho(u_{*f})^2 \tag{3}$$

where u is the velocity at a height z above the bed, κ equals von Karman's constant (0.4), and z_f is the roughness parameter. The square of the shear velocity associated with bedform resistance, u_{*f}, gives an estimate of the boundary shear stress. Velocity data from 59 separate profile at six cross-sections during the low flow experiment were fitted to Eq. (2) and shear stress was computed.

The boundary shear stress responsible for sediment transport, τ_{bs}, must be less than the other two. We have estimated τ_{bs} from a single, near-bed velocity measurement by developing an expression that predicts the hopping height of bedload particles and the resulting resistance to flow (z_o) and using this predicted roughness parameter instead of z_f in Eq. (3) (5, Dietrich and Smith, in preparation). Based on boundary layer theory we estimate the average height of the internal boundary layer near dune crests to be 4 and 3 cm at high and low flow, respectively (5). Velocity measurements closer to the bed than the heights exclude the influence of form drag over the dune. In the high flow year at eight cross-sections, a total of 116 velocity measurements at 3 cm above the bed over dune crests were used to compute τ_{bs}, whereas in the low

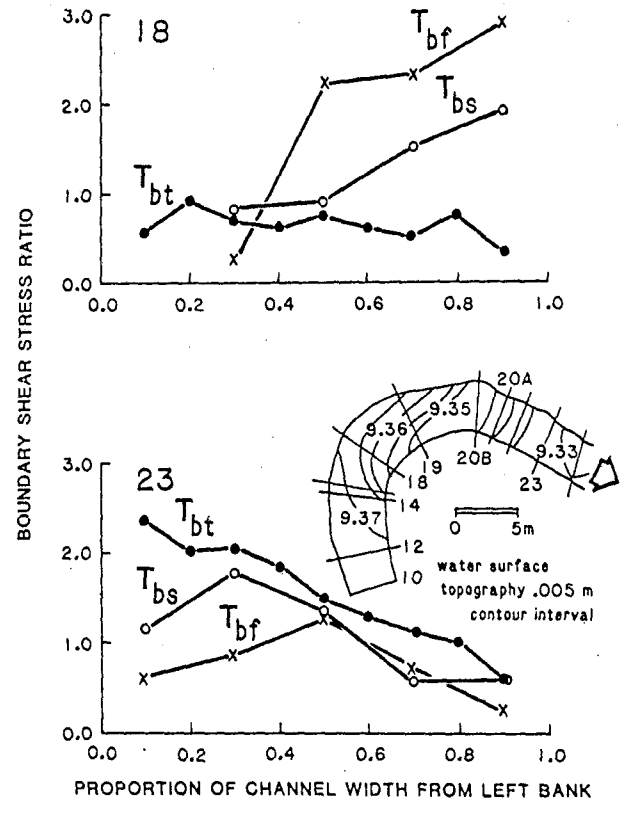

Fig. 3 - Ratio of local boundary shear stress to average for the entire reach for two sections across the Muddy Creek study bend during low flow.

flow year 92 velocity measurements taken at 2 cm above the bed at seven cross-sections were used.

Table 1 and Fig. 3 compare the magnitude and distribution of three scales of boundary shear stress for the low flow conditions. Values reported in Table 1 represent the average for the study reach. As expected, τ_{bs} is less than τ_{bf} which is smaller than τ_{bt}. An estimate of the form drag effect causing the difference between τ_{bs} and τ_{bf} can be made using the Smith and McLean equation (9):

$$\frac{\tau_{n+1}}{\tau_n} = 1 + \frac{C_D}{2\kappa^2}\frac{H}{\lambda}\left\{\ln a_3 \left[\frac{\lambda}{z_o}\right]^{4/5}\right\}^2 \tag{4}$$

Here τ_{n+1} and τ_n correspond to τ_{bf} and τ_{bs}; H and λ are the bedform amplitude and wavelength; z_o is the roughness parameter associated with τ_n; C_D is a drag coefficient equal to 0.212 for separated flow and 0.840 for unseparated flow, a_3 is a boundary layer growth coefficient equal to 0.0995, and κ is von Karman's constant. Values of H/λ and λ are given in Table 1. The roughness parameter z_o, determined empirically, was equal to about 0.01 cm. The flow separates in the lee of bedforms, so C_D = 0.212 should be used.

Table 1. - Estimates of boundary shear stress

Discharge, in cubic meters per second (1)	λ, in meters (2)	H/λ (3)	τ_{bs}, in dynes per square centimeters (4)	τ_{bf}, in dynes per square centimeters (5)	τ_{bt}, in dynes per square centimeters (6)
0.3	1.05	.07	12	22	26
1.1	1.47	.07	15	30	55

Table 2. - Predicted boundary shear stress ratios

Discharge, in cubic meters per second (1)	τ_{bf}/τ_{bs} observed (2)	τ_{bf}/τ_{bs} predicted (3)	τ_{bt}/τ_{bf} observed (4)	τ_{bt}/τ_{bf} predicted (5)
0.3	1.8	2.2	1.2	1.3
1.1	2.0	2.3	1.8	1.5

Predicted ratios (Table 2) from Eq. (4) are about 20% greater than observed for both low and high flow, a small difference considering the approximate nature of both the measurements and calculations. Eq. (4) can also be used to estimate the ratio of total boundary shear stress τ_{bt} to the shear stress corresponding to form drag over bedforms, τ_{bf}. The effects of channel curvature and the inertial terms arising from the three-dimensionality of the bar-pool topography are not included in this calculation; therefore, it should be an underestimation. In Eq. (4) we have used $H/\lambda = .016$ and .028 for low and high flow, respectively; $\lambda = 25$ m and $z_o = .135$ and .171 for low and high flow. The roughness parameter values were computed from the velocity profile data. Table 2 shows that the predicted values decrease with stage, as do the observed ones, and that they are within 20% of the observed. As expected, the high flow prediction underestimates the measured shear stress ratio. The low flow prediction, however, is slightly higher, suggesting that curvature and three-dimensional bed topography effects are smaller at this reduced stage.

In Fig. 3 the ratio of observed local boundary shear stress to the average reported in Table 1 is plotted according to position across the channel for two cross-sections. In the upstream part of the bend (section 18) the pattern of cross-stream variation in total boundary shear stress, as computed from Eq. (1) differs greatly from that found for τ_{bf} or τ_{bs}. As mentioned above, the convective acceleration terms in this part of the channel are significant but have not been included in Eq. (1); inclusion of these terms would yield a different structure to the field. Some of these differences are discussed in our other paper in this volume.

Previously we have pointed out that for the high flow case as well (4), the boundary shear stress field computed from Eq. (1) and determined from near-bed velocity profiles differed considerably in the upstream part of the bend. In the downstream part of the bend, the general structure of the boundary shear stress fields are similar, although in detail important differences still exist. For example, the cross-channel position of maximum boundary shear stress is further toward the outside bank for τ_{bt} versus τ_{bs} and τ_{bs} versus τ_{bf} (Fig. 3). In addition, Fig. 3 and low flow data from other cross-sections show an outward shift through the bend of the zone of maximum boundary shear stress causing sediment transport. Similar outward shifting has been documented for the high flow case (7) and has been observed in flumes by others (8,10).

Sediment Transport

During high flow, the zone of maximum bedload transport shifted outward through the bend with the maximum boundary shear stress zone (7). Data on bedload transport at this stage are reported in the other paper by us in this volume. Bedform migration and geometry were recorded simultaneously with near-bed velocity measurements in the low-flow year. In parts of the study reach, bedform geometry was repeatedly recorded over one to two hour intervals to provide additional data from which an estimate of the bedload transport field could be made. All measurements were taken from wooden bridges placed across the channel. At eight sections, a total of 237 bedform migration observations were used to construct the bedload transport field.

As in the high flow case, the zone of maximum bedload transport shifted outward through the bend (Figs. 4,5). Over 80% of the bedload in transport travelled to the right (closer to the inside bank) of the centerline in the upstream part of the bend (section 14). In the downstream portion of the bend, over 50% travelled to the left (closer to the outside bank) of the centerline (section 23). Shoaling and near-bed outward flow over the point bar top, rolling and avalanching on the point face and on the cross-stream sloping avalanche faces of bedforms, and troughwise transport along obliquely-oriented bedforms all contributed to the net cross-stream transport.

The boundary shear stress responsible for sediment transport, τ_{bs}, was used in the Yalin bedload equation to compute the bedload transport field at each of eight sections in both the high and low flow cases. The average bedload transport for the eight sections was 129 and 58 gm/sec for the high and low flow, respectively. The predicted bedload transport fields for individual sections closely matched the observed at high and low flow and the average was 123 gm/sec and 60 gm/sec, respectively, less than 3% smaller than observed (Fig. 5). The data points, shown in Fig. 5, are the average of all measurements in segments 0.2 channel widths across. The structure of the bedload transport field was generally well-predicted, confirming that the bulk of the bed particles in transport must shift outward through the bend.

Although the total discharge in the channel decreased by a factor of four and the boundary shear stress reduced by one-half, the observed bedload transport rates decreased by only about 2 times, from 129 to 58 gm/sec. The data in Tables 1 and 2 and the cross-section in Fig. 2 suggest an explanation for the relatively small reduction in bedload transport. At high flow the pool is deep and the top of the point bar has aggraded sufficiently to cause net outward bedload transport. This bar-pool topography with a point bar face oblique to the mean flow direction generates a large form-drag on the flow. Large convective-acceleration force terms develop (6). Nearly one-half of the total boundary shear stress is expended on large-scale resis-

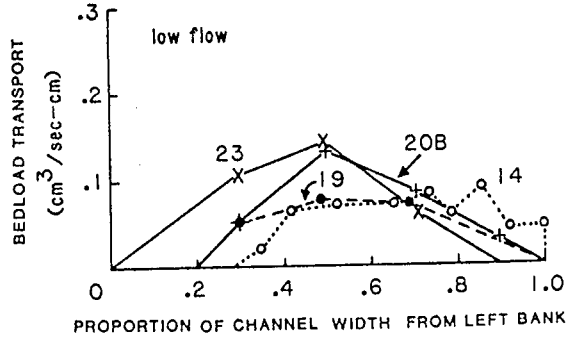

Fig. 4 - Bedload transport computed from bedform migration studies at four sections across Muddy Creek during low flow.

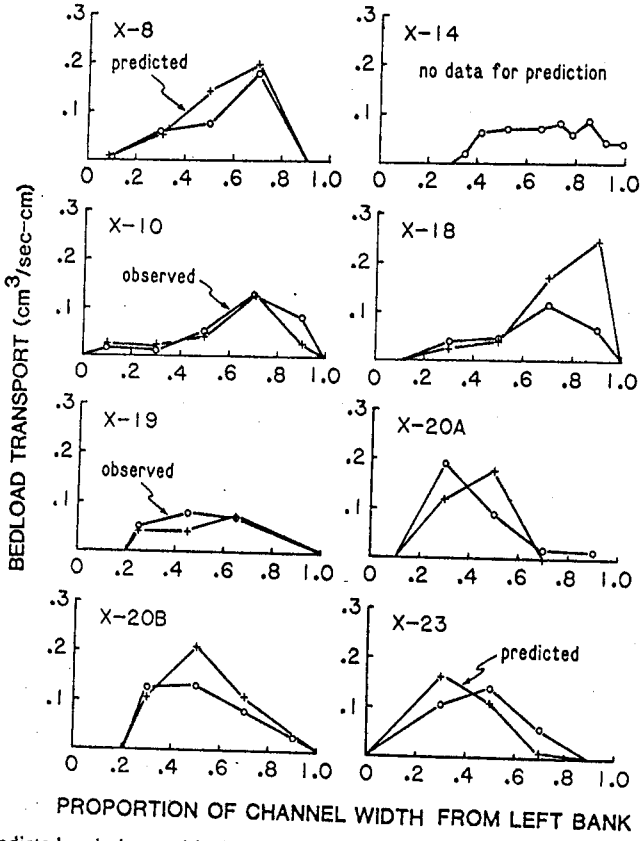

Fig. 5- Predicted and observed bedload transport fields during low flow conditions.

tance due to channel topography (including curvature). As the stage drops net transport into the pool leads to aggradation there and erosion of the point bar top. The overall form of the bar-pool topography is reduced, but the wavelength, imposed by the high flow controlled channel curvature, is maintained and to a lesser degree so is the width. In addition the mean velocity and probably the magnitude of the convective acceleration force terms are reduced. As a consequence less of the total boundary shear stress is spent on large scale form resistance and proportionately more is available for bedform and sediment transport resistance. Adjustments in bedform morphology from high to low flow produced the same ratio of crest height to wavelength (H/λ) such that the form drag loss in the high and low channels was about the same. The effects when combined led to only a 25% reduction in the boundary shear stress available for sediment transport hence a relatively small reduction in observed bedload transport.

Conclusion

In cases where the bed morphology in a river meander is in near equilibrium with the discharge, the general patterns of boundary shear stress and bedload transport at high and low flow are essentially the same. The bedload transport maximum shifts from near the inside bank toward the outside bank, tracking the outward shifting zone of maximum boundary shear stress. Similar observations were made by Hooke (8) in his study of boundary shear stress and bedload transport in a laboratory river meander.

Important morphological adjustments must occur during a stage change because of topographically-induced convergences or divergences of sediment transport associated with downstream variation of the boundary shear stress. During stage decline these imbalances will lead to deposition in the pool and erosion of the point bar such that the average form of the cross-section tends to be preserved. The reduced form resistance may lead to relatively small changes in the boundary shear stress causing bedload transport. It is now common practice to incorporate a procedure for computing the resistance due to mobile bedforms when attempting to compute the bedload transport or channel depth in a reach of river based on average channel properties (3). Our observations suggest that in a sand-bedded river, bar-pool topography exerts a considerable form drag at high flow, but at low flow, due to morphologic adjustments, this resistance may be much less significant. This stage dependent large-scale form resistance also should be accounted for in bedload transport calculation procedures.

Acknowledgements

Field work was made possible by assistance from Leslie Reid, Steve McLean, Mary Power, Wray Smith, Rich Spicer and Pat Irle. Floyd Bardsley drafted the figures and Korda Cordes thoughtfully typed the manuscript. Our research was supported in part by the Geological Society of America and NSF Grant ENG 78-16977.

Appendix - References

1. Anding, M.G. and Pierce, III, P.W., "Some Relations of Energy, Roughness, and Channel Geometry in the Lower Mississippi River", *Proceedings of the XIIth Congress of the International Association for Hydraulic Research,* Vol. 1, No. A48, 1967, pp. 389-397.
2. Anding, M.G., "Hydraulic Analysis of Mississippi River Channels, Miles 373 to 603", U.S. Army Engineer District, Vicksburg, Potamology Research Project No. 10, 1965, 22 pp.
3. Brownlie, W.R., "Flow Depth in Sand-bed Channels", *Journal of the Hydraulics Division,* ASCE, Vol. 109, No. HY3, July 1983, pp. 959-990.
4. Dietrich, W.E., Smith, J.D., and Dunne, T., "Flow and Sediment Transport in a Sand Bedded Meander", *Journal of Geology,* Vol. 87, No. 3, May, 1979, pp. 305-315.
5. Dietrich, W.E., "Flow, Boundary Shear Stress and Sediment Transport in a River Meander", Thesis presented to the University of Washington, Seattle, Washington, 1982, in partial fulfillment of the requirements for the degree of Doctor of Philosophy.
6. Dietrich, W.E., and Smith, J.D., "Influence of the Point Bar on Flow Through Curved Channels", *Water Resources Research,* Vol. 19, No. 5, October, 1983, pp. 1173-1192.
7. Dietrich, W.E., and Smith, J.D., "Bedload Transport in a River Meander", (submitted).
8. Hooke, R. LeB., "Distribution of Sediment Transport and Shear Stress in a Meander Bend", *Journal of Geology,* Vol. 83, 1975, pp. 543-565.
9. Yalin, M.S., "An Expression for Bedload Transportation", *Journal of the Hydraulics Division,* ASCE Vol. 89, No. HY3, 1963, pp. 221-250.
10. Yen, C.L., "Bed Configuration and Characteristics of Subcritical Flow in a Meandering Channel", Thesis presented to the University of Iowa, Iowa, 1972, in partial fulfillment of the requirements for the degree of Doctor of Philosophy.